# Defense Technical Information Center Compilation Part Notice

## ADP012157

TITLE: Three-Dimensional Calculation of Field Emission from Carbon Nanotubes using a Transfer- Matrix Methodology

DISTRIBUTION: Approved for public release, distribution unlimited

This paper is part of the following report:

TITLE: Materials Research Society Symposium Proceedings. Volume 675. Nanotubes, Fullerenes, Nanostructured and Disordered Carbon. Symposium Held April 17-20, 2001, San Francisco, California, U.S.A.

To order the complete compilation report, use: ADA401251

The component part is provided here to allow users access to individually authored sections of proceedings, annals, symposia, etc. However, the component should be considered within the context of the overall compilation report and not as a stand-alone technical report.

The following component part numbers comprise the compilation report:
ADP012133 thru ADP012173

# Three-dimensional calculation of field emission from carbon nanotubes using a transfer-matrix methodology

Alexandre Mayer, Nicholas M. Miskovsky[1] and Paul H. Cutler[1]
Laboratoire de Physique du Solide, Facultes Universitaires N.-D. de la Paix, Rue de Bruxelles 61, B-5000 Namur, Belgium
[1]Department of Physics, 104 Davey Lab, Penn State University, University Park, PA 16802, U.S.A.

## ABSTRACT

We present simulations of field emission from carbon nanotubes, using a transfer-matrix methodology. By repeating periodically a basic unit of the nanotubes in the region preceding that containing the extraction field, specific band-structure effects are included in the distribution of incident states, i.e. those entering the field region. The structures considered are the metallic (5,5) and the semiconducting (10,0) single-wall carbon nanotubes. The total-energy distributions of incident states show the gap of the (10,0) and the expected flat region for the (5,5) nanotube. The field-emitted electron energy distributions contain peaks, which are sharper for the (10,0) structure. Except for peaks associated with van Hove singularities in the distribution of incident states or with the Fermi level in the case of a metallic structure, all peaks are shifted to lower energies by the electric field.

## INTRODUCTION

Like other forms of nanostructured carbon, the nanotubes [1-3] show interesting field-emission properties such as low extracting field, high current density, and seemingly long operating time. In general, the current-voltage characteristics of the nanotubes are found to follow a Fowler-Nordheim type tunneling law [4] with an emitter work function varying between 4 to 5 eV depending on the type of nanotubes. Electronic states localized near or at the very end of the nanotube influence the current emission profile [5]. The localized states are relatively well documented for various kinds of tube termination [6-9]. Such localized states can be induced by the extracting electric field, as shown by recent *ab-initio* calculations [10].

To study field emission from carbon nanotubes, we used the transfer matrix technique developed in previous publications [11-13]. From a given three-dimensional potential-energy distribution (describing two biased electrodes), this methodology predicts the corresponding emitted current. For this specific application, the potential energy was calculated using for the first time the Bachelet etal pseudopotentials [14]. In addition, in order to reproduce band-structure effects in the distribution of incident states, a basic unit of the carbon nanotubes was repeated periodically, in an intermediate region between the supporting metal substrate and that containing the extraction field.
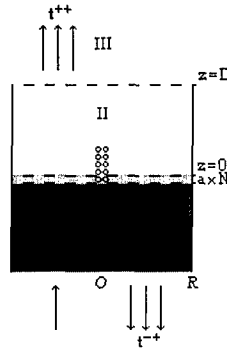
**Figure 1**. Geometry of the situation considered. Region I ($z \leq -a.N$) is a perfect metal. The intermediate region $-a.N \leq z \leq 0$ contains $N$ periodic repetitions of a basic unit of the nanotube. Region II ($0 \leq z \leq D$) contains the part of the nanotube subject to the electric field. Region III ($z \geq D$) is the field-free vacuum. The arrows in the Regions I and III symbolize scattering solutions, with a single incident state in Region I and the corresponding reflected and transmitted states (whose coefficients are contained in the transfer matrices $t^{-+}$ and $t^{++}$ respectively).

## THEORY

The geometry considered in this paper is that depicted in figure 1. The emitting nanotube stands in a region (Region II, $0 \leq z \leq D$) between a supporting metal substrate (Region I, $z \leq -N.a$) and the field-free vacuum (Region III, $z \geq D$). An electric bias $V$ is established between the two limits of Region II. The intermediate region $-a.N \leq z \leq 0$ contains $N$ periodic repetitions of a basic unit of the nanotube.

The potential energy in Region II is calculated essentially by using techniques of Ref. [11], with a pseudopotential for the ion-core potential. For this ion-core contribution, we used the expression given in Ref. [14] for the $l=1$ states. This choice is justified by the fact that the electronic current in nanotubes is due to $\pi$ electrons. The atomic orbitals, representative of the 4 valence electrons of each carbon atom, are represented here by the sum of two Gaussian distributions $\Psi = A\left(\exp(-\alpha_1 r^2) + \exp(-\alpha_2 r^2)\right)$, where the two parameters $\alpha_1 = 0.35/a_0^2$ and $\alpha_2 = 1.40/a_0^2$ ($a_0$=Bohr radius) are those recommended in Ref. [14]. These electronic densities are displaced from the nucleus positions by $\Delta r$ quantities, which are related to the dipole $p$ of the corresponding carbon atoms by $p = -4e\Delta r$. These dipoles are those induced by the extraction field and take account of dipole-dipole interactions. They are calculated by using the techniques of Ref. [12] for an anisotropic polarisability with radial and transversal components of 3 and 0.865 Å$^3$ respectively [15]. The electronic exchange term is evaluated using the Local Density Approximation $\frac{4}{3} C_X \rho^{1/3}$ (with $C_X = -\frac{3}{4} \frac{e^2}{4\pi\varepsilon_0}(\frac{3}{\pi})^{1/3}$ and $\rho$ the local electronic density)[11].

To compute electronic scattering from the supporting metal (Region I) to the vacuum (Region III) by taking account of all three-dimensional aspects of the potential barrier in the intermediate regions, we used the transfer-matrix technique developed in previous publications

[12-13]. In this formulation, the scattering electrons remain localized inside a cylinder of radius $R$ in the regions preceding the vacuum Region III ($R$ is much larger than the nanotube radius). The wave function is expanded in terms of basis states

$$\Psi_{m,j}^{I,\pm} = A_{m,j} J_m(k_{m,j}\rho)\exp(im\varphi)\exp(\pm i\sqrt{\tfrac{2m}{\hbar^2}(E - V_{met})}z)$$ in the Region I and

$$\Psi_{m,j}^{D,\pm} = A_{m,j} J_m(k_{m,j}\rho)\exp(im\varphi)\exp(\pm i\sqrt{\tfrac{2m}{\hbar^2}Ez})$$ in the anode plane $z=D$. Here the $\pm$ refers to the propagation direction relative to the $z$-axis, which is oriented from Region I to region III. The $A_{m,j}$ are normalization coefficients and $V_{met}$ is the potential energy in the metal. The methodology then provides the amplitudes of the reflected states $\Psi_{m,j}^{I,-}$ and transmitted states $\Psi_{m,j}^{D,+}$ corresponding to single incident basis states $\Psi_{m,j}^{I,+}$ in the metal (see figure 1 for a schematic representation). Total current densities result then from the contribution of all solutions associated with a propagative incident state in the metal.

## RESULTS

The two structures considered in this paper are the armchair (5,5) and zigzag (10,0) nanotubes. To reproduce the energy distributions associated with the band structure of carbon nanotubes, $N$=16 repetitions of a basic unit of the corresponding nanotubes were inserted between the metal in Region I and the beginning of the potential barrier at $z=0$. Calculations show that 16 repetitions are sufficient to reproduce the gap of the (10,0) and the metallic plateau of the (5,5) nanotube in the distribution of incident states. The work function $W$ of these two nanotubes have the values corresponding respectively to the middle of the gap (5.75 eV) for the (10,0) or the middle of the metallic plateau (5.25 eV) for the (5,5) structure.

An electric bias of 12 V is established between the supporting metal and the vacuum. The scattering simulations are performed by considering a confinement radius $R$ of 4.5 nm, basis states characterized by $m$ subscripts ranging from $-10$ to $+10$ and transverse wave vectors $k_{m,j}$ restricted by $k_{m,j} \leq \sqrt{\tfrac{2m}{\hbar^2}(E + \Delta E)}$ with $\Delta E = 4$ eV. It was found that the electron energies have to range over 16 eV below the top of the potential barrier to reproduce with reasonable accuracy the position and width of the gap and metallic plateau of the (10,0) and (5,5) nanotubes, respectively [16]. For this reason, the Fermi energy in the supporting metal was given the value $E_F$=16 eV– W.

### Field emission from an open (5,5) carbon nanotube

The first simulations consider an open (5,5) carbon nanotube. This armchair nanotube is metallic. We consider in the field-free region $z\leq0$ 16 units of this molecule (corresponding to 320 atoms), which are connected to 7 units (corresponding to 140 atoms) in the region $z\geq0$ where the extraction field is present. The first and last atoms in this region are then located respectively at $z$=0.061 and 1.660 nm. The radius of the tube is 0.339 nm (the radius of a $C_{60}$ molecule).

The extraction bias is 12 V and variations of the extraction field are obtained by changing the distance $D$ between the two electrodes. A section of the potential-energy distribution (corresponding to an electrode separation $D$ of 4 nm) is represented in the left part of figure 2. The nanotube acts essentially as a metallic cylinder, so its interior is nearly at a constant potential [17-18]. The carbon atoms are clearly indicated.
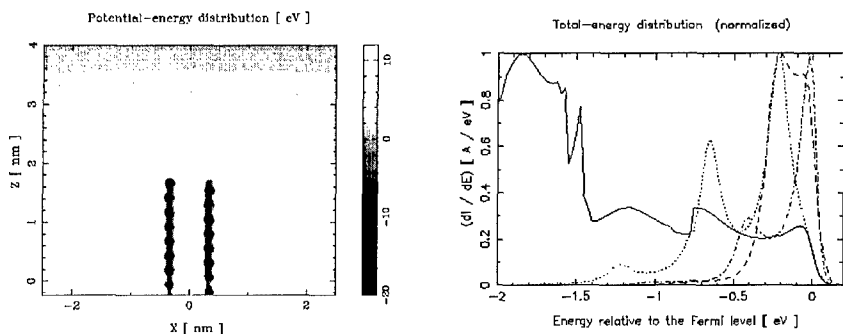
**Figure 2**. Left: Potential-energy distribution for an open (5,5) nanotube corresponding to an extraction bias of 12 V and a grid separation $D$ of 4 nm. The basic unit below $z=0$ is repeated 16 times. The contour levels correspond to integer potential-energy values. A cut-off at –20 eV is applied to improve the visibility of positive values. Right: Normalized total energy distribution of the incident states at $z=0$ (solid) and of the transmitted states at $z=D$ for an applied electric field of 0.20 (dashed), 0.25 (dot-dashed) and 0.30 V/Å (dotted). The maximal values are respectively 0.23 $10^{-3}$, 0.11 $10^{-9}$, 0.87 $10^{-7}$ and 0.81 $10^{-6}$ A/eV.

The total-energy distribution of the field-emitted electrons is illustrated in the right part of figure 2. The four curves correspond to the incident distribution at $z=0$ and the transmitted distribution at $z=D$ for an applied electric field of 0.20, 0.25 and 0.30 V/Å. The absolute values as well as the width of the distributions are increasing with the extraction field, in agreement with elementary field-emission theories [19]. In all cases, there is a significant contribution at the Fermi level (due to a higher transmission probability and a non-zero supply function). The sharp peak at the edge of the metallic plateau is a van Hove singularity [20]. The other oscillations in the distribution of incident states are due to standing waves in the nanotube. Their period tends to decrease with the number $N$ of repetitions of the basic unit.

There are well pronounced peaks in the distributions below the Fermi level. They move to the left with increasing extraction bias as a result of field penetration, which lowers the potential energy at the apex of the nanotube as well as its mean value in the whole nanotube. Similar displacements have been observed experimentally with carbon emitters [3,21]. The peaks tend to the positions observed in distribution of incident states at $z=0$. This can be understood if we still relate these peaks to standing states in the whole nanotube. At low electric field, the effective length of the nanotube associated with standing waves is larger (since including parts in Region II) so the separation between peaks is shorter. At high fields, the end portion of the nanotube no longer tends to contribute to these standing waves, since its mean potential energy differs significantly from that in the region $z \leq 0$.

Representing $\log(I/F^2)$ as a function of $1/F$ (Fowler-Nordheim plot) gives a line, whose slope indicates [1] a field enhancement factor $\gamma$ of 3.8. This small value compared to experimental data, where $\gamma$ is typically found between 500 and 800 for multiwall nanotubes [1] and around 3000 and above for single-wall nanotubes [2], is obviously due to the small aspect ratio of the nanotube used in our calculation ($L/D \sim 2.5$). This also explains why the electric field used in the calculations needs to be a factor of 1000 larger than in experimental conditions [4].
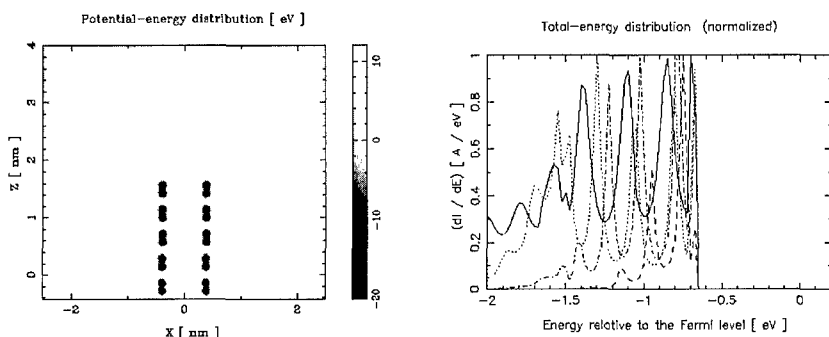
**Figure 3**. Left: Potential-energy distribution for a (10,0) nanotube corresponding to an extraction bias of 12 V and a grid separation $D$ of 4 nm. The basic unit below $z=0$ is repeated 16 times. The contour levels correspond to integer values. A cut-off at $-20$ eV is applied to improve the visibility of positive values. Right: Normalized total energy distribution of the incident states at $z=0$ (solid) and of the transmitted states at $z=D$ for an applied electric field of 0.20 (dashed), 0.25 (dot-dashed) and 0.30 V/Å (dotted). The maximal values are respectively 0.15 $10^{-3}$, 0.40 $10^{-19}$, 0.17 $10^{-15}$ and 0.37 $10^{-13}$ A/eV.

## Field emission from a (10,0) carbon nanotube

In the last simulations, an open (10,0) carbon nanotube is considered. This zigzag nanotube is semiconducting. We again consider in the field-free region $z{\leq}0$ 16 units of this molecule (corresponding to 640 atoms), which are connected to 4 units (corresponding to 160 atoms) in the region $z{\geq}0$ where the extraction field is present. The first and last atoms in this region are located respectively at $z=0.071$ and 1.633 nm. The radius of the tube is 0.391 nm. The geometrical dimensions are therefore close to those of the open (5,5) structure. The corresponding potential-energy and total-energy distributions are presented in figure 3. The carbon atoms are organized by pairs in the potential-energy representation, due to the figure passing exactly through C-C bonds that are parallel to the $z$ axis.

The total-energy distributions present a gap, which is centered at the Fermi level. The peaks are sharper than for the metallic (5,5) nanotube (thus reaching the results of Adessi etal [5]). We can see that the sharp peak at the edge of the gap (which is due to a van Hove singularity) does not move significantly with the extraction field while all the others are shifted to lower energies. As in the previous case, the peaks reach the positions observed in the distribution of incident states. A field enhancement factor of 2.5 can be derived from the slope of the Fowler-Nordheim plot (essentially revealing the field-emission process to be inefficient). This small value is a consequence of the absence of emission at the Fermi level due to the gap.

## CONCLUSIONS

Transfer-matrix calculations of field emission from carbon nanotubes were presented. With the use of pseudopotentials, the methodology takes account of band-structure effects (i.e. reproducing the gap of the (10,0) and the metallic plateau of the (5,5) nanotube in the distribution

of incident states) and of all three-dimensional details of the tunneling barrier. The total-energy distributions of both the semiconducting (10,0) and metallic (5,5) nanotubes contain peaks, which are sharper for the (10,0) structure. Except for peaks associated with the van Hove singularities in the distribution of incident states or with the Fermi level in the case of a metallic structure, all peaks are shifted to lower energies by the electric field.

## ACKNOWLEDGMENTS

## REFERENCES

[1] W.A. de Heer, A. Chatelain and D. Ugarte, Science **270**, 1179 (1995).

[2] J.M. Bonard, J.P. Salvetat, T. Stockli, L. Forro and A. Chatelain, Appl. Phys. A **69**, 245 (1999) and references therein.

[3] M.J. Fransen, Th.L. van Rooy and P. Kruit, Appl. Surf. Sci. **146**, 312 (1999) and references therein.

[4] P.G. Collins and A. Zettl, Phys. Rev. B **55** (15), 9391-9 (1997).

[5] Ch. Adessi and M. Devel, Phys. Rev. B **62** (20), 13314-7 (2000).

[6] T. Tamura and M. Tsukada, Phys. Rev. B **52** (8), 6015-26 (1995).

[7] D.L. Carroll, P. Redlich, P.M. Ajayan, J.C. Charlier, X. Blase, A. De Vita and R. Car, Phys. Rev. Lett. **78** (14), 2811-4 (1997).

[8] A. De Vita, J.Ch. Charlier, X. Blase and R. Car, Appl. Phys. A **68**, 283 (1999).

[9] Ph. Kim, T. Odom, J.L. Huang and C.M. Lieber, Phys. Rev. Lett. **82** (6), 1225–8 (1999).

[10] S. Han and J. Ihm, Phys. Rev. B **61**, 9886 (2000).

[11] A. Mayer, P. Senet and J-P. Vigneron, J. Phys. Condens. Mat. **11** (44), 8617-31 (1999).

[12] A. Mayer and J.-P. Vigneron, Phys. Rev. B **56** (19), 12599-607 (1997).

[13] A. Mayer and J.-P. Vigneron, J. Phys. Condens. Mat. **10** (4), 869-81 (1998) ; Phys. Rev. B **60** (4), 2875-82 (1999) ; Phys. Rev. E **59** (4), 4659-66 (1999) ; Phys. Rev. E **61** (5), 5953-60 (2000).

[14] G.B. Bachelet, H.S. Greenside, G.A. Baraff and M. Schluter, Phys. Rev. B **24** (8), 4745-52 (1981).

[15] P.A. Gravil, Ph. Lambin, G. Gensterblum, L. Henrard, P. Senet, A.A. Lucas, Surf. Sci **329**, 199 (1995).

[16] R. Moussaddar, A. Charlier, E. McRae, R. Heyd and M.F. Charlier, Synthetic Metals **89**, 81-86 (1997).

[17] A. Maiti, C.J. Brabec, C. Roland and J. Bernholc, Phys. Rev. B **52** (20), 14850-8 (1995).

[18] L. Lou and P. Nordlander, Phys. Rev. B **52** (3), 1429-32 (1995).

[19] R.H. Fowler and L. Nordheim, Proc. R. Soc. London, Ser. A **119**, 173 (1928) ; R.H. Good and E. Muller, Handb. Phys. **21**, 176-231 (1956).

[20] J.M. Ziman, *Principles of the theory of solids* (The University Press, Cambridge, 1964) p. 46.

[21] K.A. Dean, O Groening, O.M. Kuttel and L. Schlapbach, App. Phys. Lett. **75** (18), 2773-5 (1999).